Indonesian Journal of Pharmacy

VOL 34 (2) 2023: 291–301 | RESEARCH ARTICLE

Formulation and Evaluation of Nano-Zinc and *Annona Muricata* Extract Particles Loaded Topical Gel

Nuniek Nizmah Fajriyah[1], Slamet S[2], Urmatul Waznah[2], Dwi Bagus Pambudi[2], Fridiana[2], Eka Dian Safitri[2], Fahrun Nur Rosyid[3], Muhtadi[4]* and Eko Mugiyanto[2,5]

1. Department of Nurse, University of Muhammadiyah Pekajangan Pekalongan, Indonesia, 51172
2. Department of Pharmacy, University of Muhammadiyah Pekajangan Pekalongan, Indonesia, 51172
3. Department of Nurse, University of Muhammadiyah Surakarta, Indonesia, 57169
4. Department of Pharmacy, University of Muhammadiyah Surakarta, Indonesia, 57169
5. Reka Institute of Science and Technology, Indonesia

Article Info

Submitted: 06-10-2022
Revised: 28-04-2023
Accepted: 15-05-2023

*Corresponding author
Muhtadi

Email:
muhtadi@ums.ac.id

ABSTRACT

A scientific method is essential for phytochemists to deliver active ingredients in a consistent manner. It can be accomplished through the development of novel drug delivery systems for active compounds in plant. The objective of the study is to develop nanoparticles loaded topical gel from *Annona muricata* leaves extract and nano-zinc in order to improve the therapeutic potential of *A. muricata* leaves extract and to provide greater targeted delivery. The active components were extracted by cold maceration of *A. muricata* leaves using ethanol and then converted into polymeric nanoparticles by gelation method based on electrostatic interaction between the Hydroxyl Amine on Chitosan and a cluster of negative charge from the polyanion NaTPP. Zinc oxide nanoparticles were formulated by precipitating zinc acetate with sodium hydroxide. They were incorporated into Carbopol-940 to generate the gel matrix. The result demonstrated that polymeric nanoparticles are nearly spherical of 358.45 ± 11.3 nm in size and in the range of PDI value of 0.440-0.812. The gel exhibits high viscosity, neutral pH, and acceptable spreadability. In addition, a stability assay demonstrates that it has chemical stability and does not cause skin irritation, making it appropriate for nanostructured hydrogel for topical delivery.

Keywords: drug delivery systems, nanotechnology, *Annona muricata*, polymeric nanoparticles, hydrogel

INTRODUCTION

Since ancient times, natural products have been widely used to treat various diseases. However, their preparation requires a variety of constituents that work synergistically to ensure their efficacy (Ansari, *et al.,* 2012). Yet approximately eighty percent of the world population use herbal medicines for primary health care. Herbal medicines are widely available, affordable, time-tested, and considered safer than the majority of modern synthetic drugs (WHO, 2019). To increase patient compliance and to prevent unnecessary repeated administration, phytotherapeutics require a scientific approach to deliver the constituents on a sustainable basis. Among the approaches is the development of novel drug delivery systems (NDDSs) for the delivery of herbal constituents. In addition to minimizing the need for repeated administration to counter non-compliance, NDDSs also help improve therapeutic value by lowering toxicity and increasing bioavailability (Sungthongjeen, *et al.,* 1999). Integration of herbal extracts into novel formulation systems has certain added benefits, including bulk dosing and less absorption, which entice many major drug companies.

Nanomedicine refers to the application of nanotechnology for treating, diagnosing, monitoring, and controlling biological systems (Moghimi *et al.,* 2005). The nanocarriers are made of non-hazardous materials such as synthetic biodegradable polymers, lipids, and polysaccharides (Patra *et al*., 2018). Meanwhile, the efficacy of herbal medicines relies on the overall feature and synergy of their active constituents. Each active constituent has a critical part and is interconnected with others. Nevertheless, most herbal drugs are insoluble, resulting in lower

bioavailability and higher systemic clearance, requiring repeated administration or higher doses, and making them a poor candidate for therapeutic use (Kesarwani *et al.,* 2013). Recently, nanoparticles received considerable attention as they potentially increase solubility; bioavailability; protection against toxicity; pharmacological activity; stability; tissue macrophage distribution; sustained delivery; and protection against physical and chemical degradation of herbal drugs (Khan *et al.,* 2019). Compared to synthetic pharmaceutical agents, herbal medicines offer more affordable wound healing products with higher safety from hypersensitive reactions (Moghadamtousi *et al*., 2014). *A. muricata*, also widely recognized as soursop or graviola, belongs to the *Annonaceae* family (Mugiyanto, Cahyanta, Putra, Setyahadi, & Simanjuntak, 2019). The leaves of this tropical fruit tree have been widely used to treat skin diseases and abscesses (Moghadamtousi *et al*., 2015). However, only few studies discuss the use of graviola as an active component of topical medication and herbal nanoparticle formulation.

In the last century, many studies emphasize the significance of zinc concentrations for healing wounds in patients with thermal burns or exposure to surgical stress (Henzel, *et al*., 1970). Meanwhile, despite the vital function of zinc in bone metabolism, growth, development, immunological system, and central nervous system (Roohani, *et al*., 2013), the total amount of zinc in the human body is less than 50 mg per kg body weight. Delayed wound healing is associated with zinc deficiency hence therapeutic modality is required (Gupta, *et al*., 2014). The present study investigates the potential of the NDDSs combination of *A. muricata* leaf extract and zinc oxide nanoparticles to accelerate wound healing.

MATERIALS AND METHODS

Preparation and characterization of *A. muricata* leaf extract

The leaves were collected from Pekalongan Regency, Central Java, Indonesia. They were dried, ground into powder, and subjected to 90% ethanol extraction. Separately, 500 g of powder was macerated in 70% ethanol. After 24 h cold maceration, the extract was filtered using cellulose membrane. The ethanolic filtrate was concentrated by distilling off the solvent on a water bath at a temperature not exceeding 60^{o}C until one-third remained for further tests, henceforth referred to as **ALE**.

Total Flavonoid

Prior the subsequent chemical and formulation evaluation, the standardization procedure was carried out (Kalaiselvi *et al*., 2012). Based on a technique developed by Daud *et al*., phytochemical screening was done to determine the presence of secondary metabolites such as flavonoids, glycosides, saponins, terpenoids, and steroids in ALE (Najihah, *et al*., 2016).

The flavonoid content of ALE was done determined using a colorimetric method developed by Chern *et al*. (Chang, *et al*., 2002). The calibration curve was prepared using quercetin. Initially, 10 mg of quercetin was dissolved in 70% ethanol and subsequently diluted to obtain different concentrations of 5, 25, 50, and 100µg/ml. Separately, 1.5 mL of 95% ethanol, 0.1mL of 10% aluminum chloride, 0.1mL of 1M potassium acetate, and 2.8mL of distilled water were mixed with the diluted standard solution (0.5mL). After incubation at room temperature for 25 min, the absorbance of the reaction mixture was measured at 415 nm using a Shimadzu UV-1280 spectrophotometer (Kyoto, Japan). Total flavonoid levels were calculated by integrating the calibration curve of a standard quercetin solution with various concentration of 4, 8, 12, 16, and 20µg/ml. The total flavonoid content of ALE was expressed as mg quercetin equivalent (QE)/g of dried extract (mg/g).

Total phenolic

The total phenolic content of ALE was evaluated using the Folin-Ciocalteu method using gallic acid as a reference to obtain different concentrations of 5, 50, 100, 250, and 500 µg/ml (Padmini, *et al*., 2015). Gallic acid and Folin-Ciocalteu were mixed and incubated at room temperature for 15 min. A Spectra max microplate reader was used to measure the absorbance at 760nm. The ALE (0.5g) was diluted with water to obtain 10mg/ml. Subsequently, 0.5 ml of ALE was reacted with 5ml of Folin-Ciocalteu reagent. After incubation, the absorbance was identified. For each concentration, three replicates were performed. Using an equation derived from the standard gallic acid curve, total phenolic content of the ALE was calculated and expressed as mg of gallic acid equivalent (GAE)/g of extract.

Preparation of nanoparticles loaded topical gel (gel-based)

Preparation of ALE nanoparticle (nALE)

Chitosan nanoparticles were prepared by ionic gelation of chitosan with sodium

tripolyphosphate (NaTPP) anions (Iswanti *et al*., 2019). Initially, 0.16 g of low molecular weight chitosan (MW ~15,000, polyscience, Warrington, PA, USA) was dissolved in aqueous solution of acetic acid 1% (v/v). The chitosan solution was stirred at 60°C for two h using a paddle stirrer to form a viscous solution. The solution pH was adjusted at 4.7–4.8. An amount of 0.04 g of sodium tripolyphosphate (TPP) (Wako Pure Chemical Industries, Osaka, Japan) was dissolved in 20ml of distilled water. Subsequently, 0.5 g ALE was added into NaTPP solution and stirred for 1 h. After all the components were mixed with the previously prepared chitosan solution, it was stirred for 30 min. The generated ALE nanoparticle (nALE) was stored at 4°C for further test.

Preparation and characterization of zinc nanoparticles (nZPs)

The preparation of nano-Zinc method was adopted from Zhiguo *et al*. (Wang, *et al*., 2018) with slight modification. Zinc acetate and sodium hydroxide were the starting materials for the synthesis of nZPs. An amount of 4.16 g zinc acetate was dissolved in 100 mL of deionized water. A mother solution as alkali solution prepared from sodium hydroxide (0.8 N) was gently dropped onto zinc acetate solution with an approximate rate of 5 mL/min to make a solution of pH 12. A magnetic stirrer cum heater for constant stirring was used at 50-60°C. The precipitate formed from the reaction between zinc acetate and sodium hydroxide solution was collected by filtering and rinsing it with 96% ethanol for three times. The final yield was obtained after 8 h of oven-drying at 60°C.

To confirm the formation of zinc oxide nanoparticles and the absence of $Zn(OH)_2$ in the precipitate obtained from the synthesis process, X-ray diffraction (XRD) was used to provide information on the crystal structure of the nanoparticles. An XRD holder was used to measure Zn(OH)2 after the substance was prepared and finely pulverized. After the holder was fixed into the XRD diffractometer, the diffraction parameters such as scanning angle, X-ray radiation direction, and wavelength were set. The holder was then moved to scan the diffraction pattern while the XRD software analyzed the peaks. The existence of crystals in the sample was indicated by these peaks. Subsequently, the peaks were compared to the reference of crystal structure databases (i.e., PDF or ICDD). The matching procedure revealed the details about the sample's crystal structure.

Preparation of the gel

The ALE and nALE were added into Carbopol-940 to obtain a final product in the form gel (Figure 1). The gel preparation was done by mixing two active compounds: nALE and nZPs. Following vigorous stirring, 10 g of glycerin was added as a humectant after dissolving 0.5 g of Carbopol-940 (Merck) into 50 ml of distilled water to make the gel-based ingredient. To balance the pH of the liquid, 1 g of triethanolamine was added and 0.1 g of methylparaben was dissolved into the mixture as a preservative. The result was cooled until it was solidified into a homogeneous mass. Subsequently, it was diluted in 1 ml of 6N sodium hydroxide and then 100mg of nALE and gel base were added to produce 100ml of gel.

Characterization of gel

Droplet size and zeta potential

The HORIBA SZ-100 Nanoparticle Analyzer was used to measure the particle size. The time dependent intensity fluctuation of the scattered light induced by Brownian motion was used to estimate the diffusivity of suspended particles. The surface morphology of gel was examined using scanning electron microscopy (SEM) (JEOL, JSM 50A, Tokyo, Japan). A suitable amount of colloidal dispersion of polymeric nanoparticle was mounted onto metal (aluminium) using double-sided adhesive tape and then fractured with a razor blade.

pH

The pH was determined by a digital pH meter (Systronics digital pH meter 335).

Spreadability

The spreadability of the gel was determined by measuring the spreading diameter of the gel between two glass plates for 1 min (Batheja, *et al*., 2011).

Viscosity

The viscosity of the gel was measured using a Brookfield DV-II+ Pro Viscometer at 60 rpm on Spindle No. 4.

Cross-linking

The Fourier Transform Infrared/FTIR (Shimadzu IRSpirit) was employed to analyze cross-linking between the base and the nZPs.

Total flavonoid in the gel

The active compounds of ALE were tested by determining the flavonoids in the gel. The UV-Vis Spectrophotometer was used to analyze the chemical properties of the gel. Initially, 1000 µg/ml of the sample was diluted in 70% ethanol.

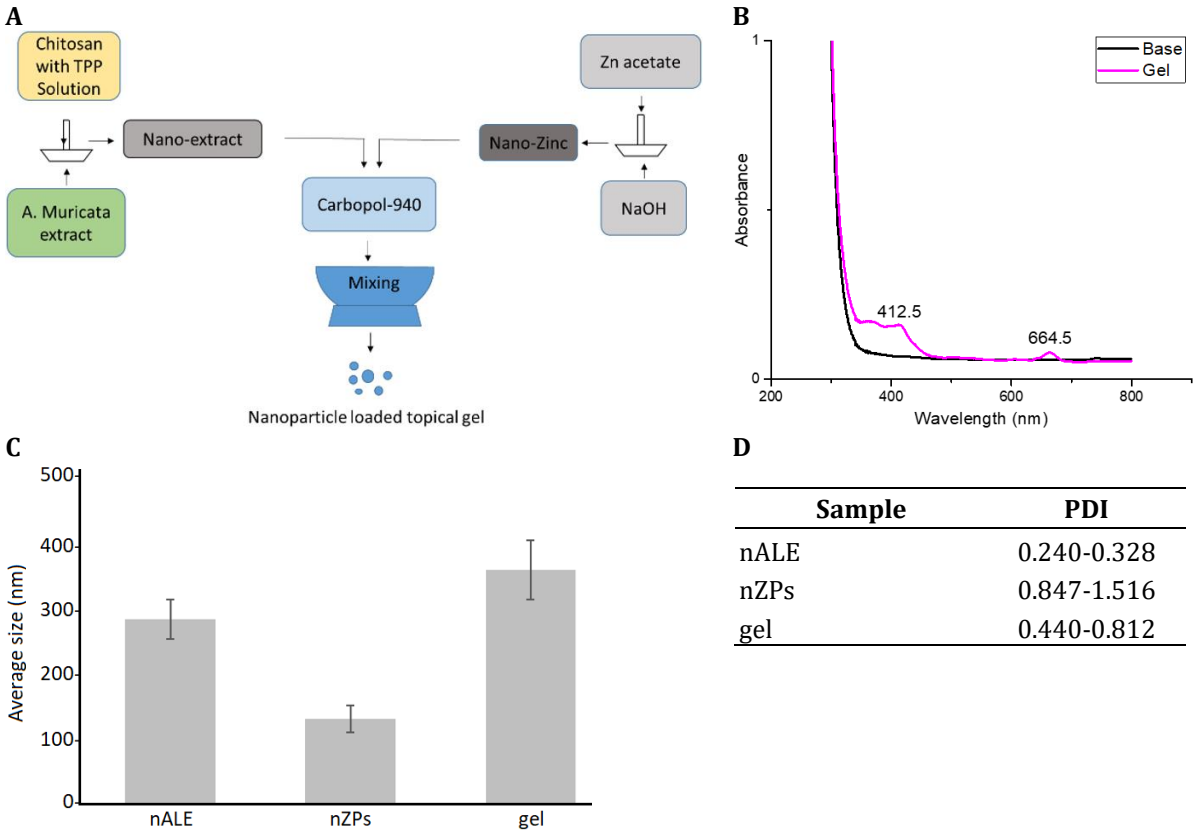

Sample	PDI
nALE	0.240-0.328
nZPs	0.847-1.516
gel	0.440-0.812

Figure 1. Nano-hydrogel study and characterization of each component: (A) Nano-hydrogel with carbopol-940 as the base, (B) The Normalized UV-Vis profile of ALE and base in the gel, (C) The diameter of nanoparticles of each component (Means ± S.D., n = 3), (D) The polydispersity index (PDI) of each component of the gel.

The solution was then evaluated using a UV-Vis Spectrophotometer at wavelength of 412.5 nm (Figure 1B).

Physical and chemical stability

Monitoring different changes in the bond structures of compounds under heat stress using FTIR spectroscopy can provide information about the products. Thermal stability is a key parameter to analyze a product (Ogbu & Ajiwe, 2016). In the present study, the chemical stability of the gel was tested using FTIR (Shimadzu IRSpirit) to identify the functional group of active components based on the peak value in the region of infrared radiation. An appropriate amount of sample was placed directly on the germanium pieces, and the data of infrared absorbance collected over the wave number from 4000 cm^{-1} to 675 cm^{-1} were recorded. The chemical and physical stability tests were conducted concurrently for three months.

Dissolution testing

pH 7.4±0.05Phosphate buffered saline (±0.05 M, pH 7.4) was used for the dissolution test (Gato *et al*., 2020). The conditions included: 100 rpm using the paddle over disc and dissolution medium of 500mL solution (Japanese Pharmacopoeia) at 37C. The paddle over disc (Guoming RC-3 Dissolution tester) had met the USP Apparatus 5 requirements. Hairless mouse skin was placed on 2.0 g of gel and punched out into a metal circle of 23mm in diameter. An amount of 10 ml of solution was collected at 0 and after 15, 30, 45, and 75 min, followed by the refill of the same quantity solution. Quercetin was selected as the reference substance with a peak wavelength of 255 nm for quantitative analysis.

Irritation assay

Approximately 2-3.5 kg weighted male healthy rabbits were subjected to the skin irritancy test. Formerly, the involvement of animals in the

present study had been approved by the Ethical Com mittee of Universitas Ahmad Dahlan. Two treatment groups: control group and sample group, were set with three rabbits for each group. The acclimation of rabbits required shaving them on the back with an area of 8x4 cm divided into 4 parts. The gel was smeared on the shaved area. It was then covered with gauze and plaster. After 24, 48, and 72 h, it was re-opened rinsed with water. Meanwhile, after 40 min, the occurrence of erythema and oedema was observed. Any visible changes, including erythema (redness) and oedema (swelling), on the skin surface were observed (Joshi & Patravale, 2006; Robinson *et al*., 1991). The data were then examined to determine the primary irritation index (PII).

RESULT AND DISCUSSION

Phytochemical properties and chemical composition of ALE

The ethanolic extract of *A. muricata* was greenish with the percentage of yield of 6%. Both specific and non-specific parameters were observed (Table I). A prior study found two major components in *A. Muricata* extract, i.e., quercetin-3-O-rutinoside and kaempferol-3-O-rutinoside—which belong to the flavonoid group (Kim *et al*., 2016). Additionally, the phytochemical analysis also confirmed the flavonoid content in the ALE (Table S1). These findings verified previous research by Kingsley and Paulinus (Agu & Okolie, 2017).

Table I. Specific and non-specific properties of ALE

No	Parameters	Description
1	Physical appearance	semi-solid
2	Color	dark brown
3	Odor	not typical
4	Taste	bitter
5	Water content (%)	6.17-6.56
6	Total ash content (%)	4.01-4.75
7	Acid insoluble ash (%)	2.34-2.50
8	Loss on drying (%)	10.15-10.53

The standard quercetin and gallic acid curves (Figure S1 and Figure S2), with average absorbance values for various reference standard concentrations. The chemical content assay showed that the ALE contained a total flavonoid of 1214±0.9 mg QE/g and total phenolics of 48.81±1.6 mg GAE/g.

Characteristics of gel

We successfully prepared nanoparticles of nALE and ZNPs into the carbopol-940 gel matrix. The appearances of the gel (Figure S3): with and without the particularizing approach. The gel was greenish in color, translucent, homogeneous, smooth, and stable (Table II). In addition, neither crystals nor phase separation were observed in the gel system. The pH was in the acceptable range for skincare. shows The gel did not exhibit irritation response (Table S2) (Figure S4), while (Table S3) the category of irritation response and level**.** The spreadability of gel formulations exhibited a slip-and-drag phenomenon.

Table II. Physical properties of the gel

Parameter	Description
Colour	Greenish, translucent
Appearance	Transparent
Homogeneity	Highly homogeneous (no crystals observed)
Texture	Smooth
Stability	No phase separation
pH	6.0 ± 0.02
Viscosity	68.06 dpas
Spreadability	3.1-3.5 cm (50-100 g)
Adhesion	4 seconds

Total flavonoid content of the gel

The standard curve for total flavonoids of the gel was made using quercetin standard solution under the same procedure described previously (Figure S5). After integrating the absorbance of sample into the calibration curve, the total flavonoid of the gel was 2.08±0.9 mg QE/g. The result showed that the total flavonoid was around one-tenth of the initial concentration.

Particle size

Chitosan nanoparticles with an average size of 282.75 ± 12.6 nm were synthesized using the ionic gelation method (Figure 1 C). The average size of the gel was larger than the size of single component, suggesting the binding abilities of chitosan to both nALE and ZNPs. Additionally, the polydispersity index (PDI) of the gel was in the range from 0.440 to 0.812 (Figure 1D). This index is an indicator of the size distribution of polymer molecular weight and colloidal system, as well as the dispersion stability of nanoparticles.

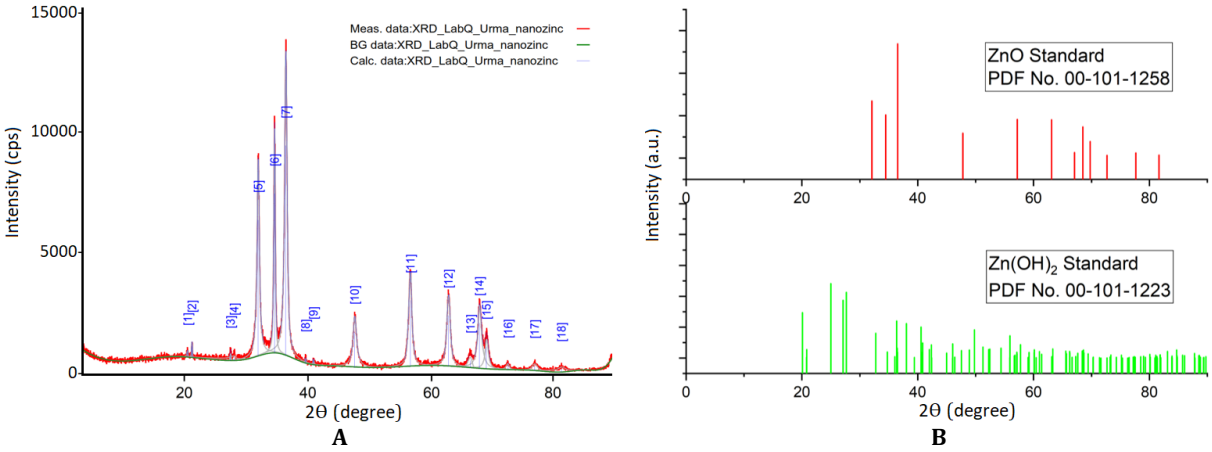

Figure 2. The XRD spectra of: A) sample (nZPs), and B) two standards: nZPs (PDF No. 00-101-1258) and Zn(OH)2 (PDF No. 00-101-1223).

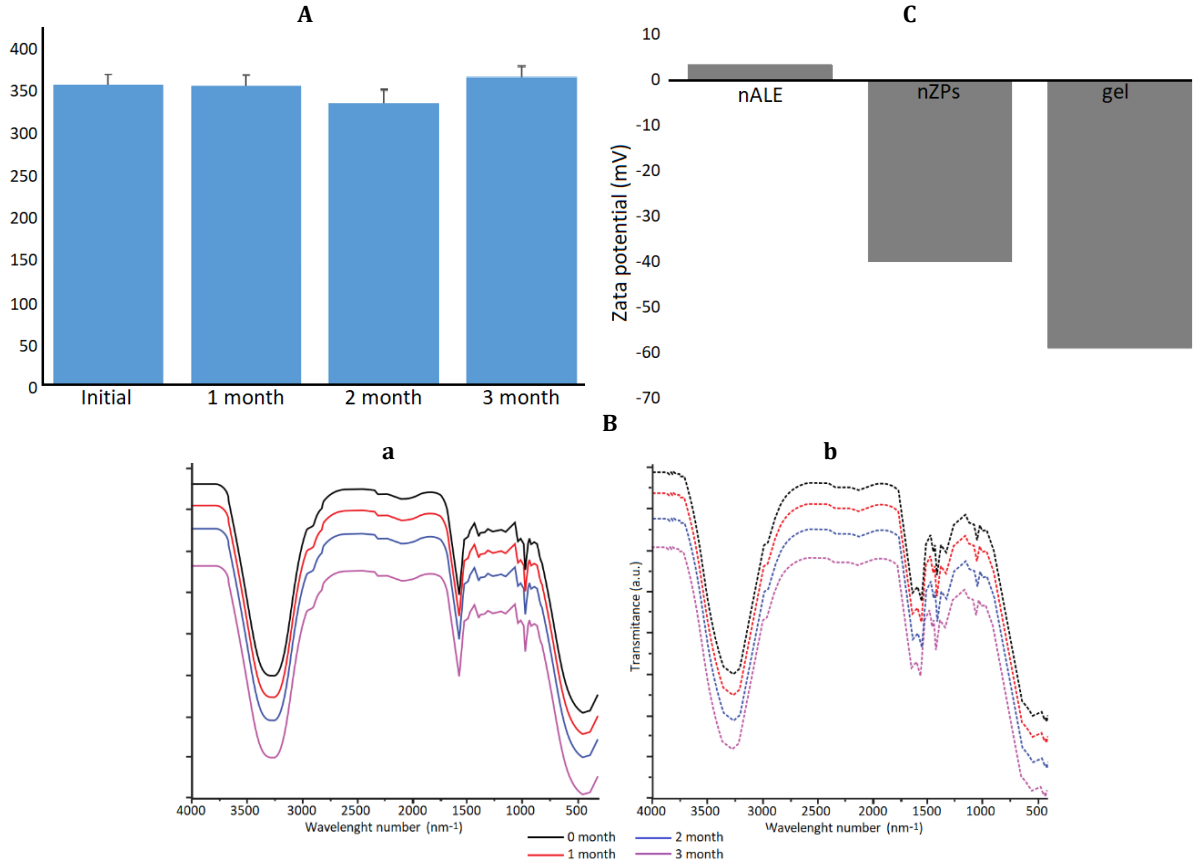

Figure 3. (A) Gel stability during the three months of observation: the average diameters of the gels are not significantly different at 5% level of significance, (B) The chemical stability of ALE: (a) compared to ALE incorporated into the gel, (b) after 3 months of monitoring under infrared radiation, (C) the zeta potential of each component of the gel.

High PDI value indicates the high variability, whereas low PDI value indicates the homogeneity of nano-particle size in suspension (Abdellatif, *et al*., 2018).

nZPs precipitation

Several analytical methods can be used to determine the existence of $Zn(OH)_2$ precipitates. In this study, X-ray diffraction (XRD) analysis was done to determine the crystal structure of $Zn(OH)_2$ (Figure 2). The XRD spectra revealed that both nZPs and $Zn(OH)_2$ had unique peaks at different 2-theta degrees. The 2-theta degree measures the angle of diffraction, which is determined by the interatomic distance of the crystal lattice. By comparing the peaks of nZPs and $Zn(OH)_2$, it is possible to identify the presence of ZnO precipitates.

The XRD spectra indicated the presence of ZnO precipitates in the sample. This can be seen at 2-theta degree values of 31.78, 34.49, and 36.32°. These values correspond to the characteristic peaks of ZnO standard (PDF No. 00-101-1258) of 32.07, 34.47, and 36.53°. Therefore, the presence of ZnO precipitates in the sample was verified. The intensity of the peaks were compared to the intensity of other peaks in the spectrum to determine the percentage of ZnO precipitates in the sample (Talam *et al*., 2012).

Gel stability

Stability test was performed on the gel formulation stored at 40°C and 75% relative humidity for three months based on the ICH guidelines. Particle size was examined to determine the possibility of aggregation in the formulation (Figure 3A). Meanwhile, physical appearance was indifferent from that of the initial formulation.

Fourier transform infrared spectrometry (FTIR) is a psychochemical analytical method that provides a snapshot of the metabolic composition of tissue at a given time but does not resolve the concentrations of individual metabolite (Najihah *et al*., 2016). The FTIR spectra showed that hydroxyl functional groups were strongly and widely adsorbed at 3262.75 cm^{-1}. In addition, the presence of alkenes (1634 cm^{-1}), ester (1980 cm^{-1}), aromatic ring (1590 cm^{-1}), and hydroxyl groups in the extract were identified based on the structure of annonaceous acetogenins from *A. muricata* (Figure 3B. a). The figure also showed that after three months, the FTIR spectra of the extract were still consistent. A similar result was also obtained when ALE was incorporated into the gel. The FTIR profile indicated no sign of chemical degradation (Figure 3B. b).

Zeta potential and morphology of the gel

Zeta potential is the degree of electrostatic repulsion of the dispersed system. Higher zeta potential values indicate higher dispersion stability and resistance to aggregation. The zeta potential of the prepared formulation was less than -40 mV, indicating the stability of the system, except for nALE (less than 4 mV) (Figure 3C).

The morphology of the prepared gel (Figure 4) the gel exhibited a nearly spherical shape and around 358 nm in size, which is consistent with the result obtained from the dynamic light scattering (DLS) technique.

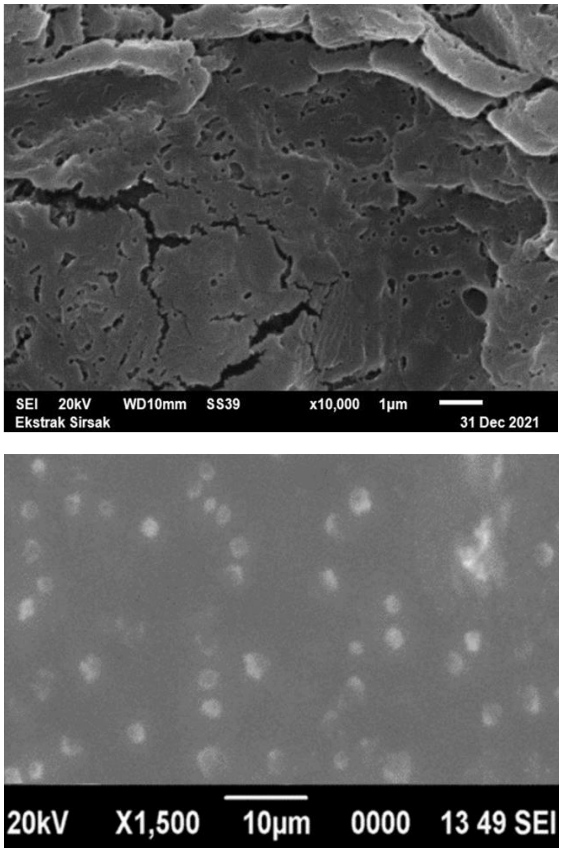

Figure 4. Scanning electron microscopy of the gel loaded with nALE and ZNPs: A) The morphology of the nanoparticle, B) nano-particles of the produced gel.

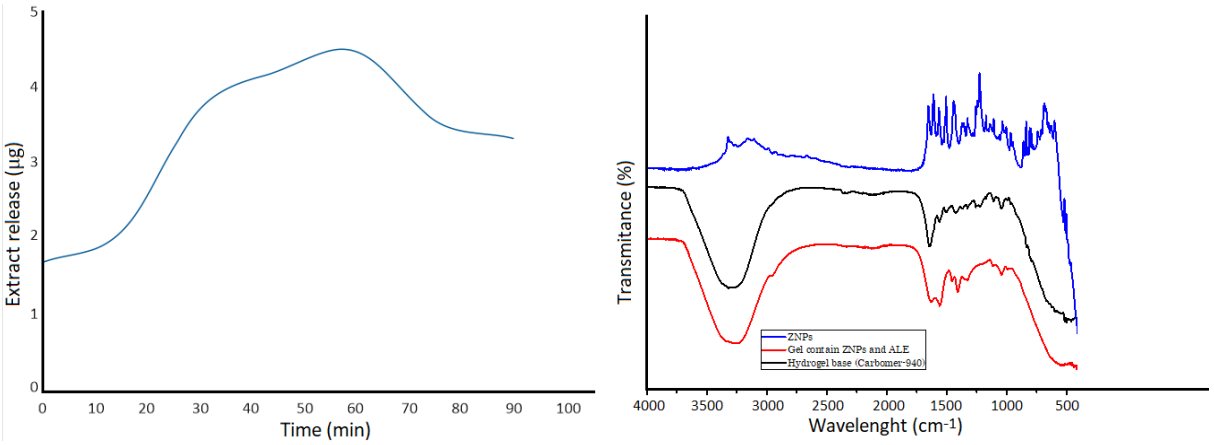

Figure 5. (A) The release profile of *A. muricata* leaf extract, (B) The FTIR profile of ZNPs, gel, and hydrogel base: the right shift at 1600 cm-1 (black) toward 1400 cm-1 (red) indicates the cross-linking between carbopol-940 and zinc acetate.

Dissolution of the gel

The profile of ALE in the gel matrix (Figure 5A) it demonstrated that the maximum release occurred after 1 h. The calibration curve (Figure 5B) shows linear response at concentration range of 2-15 µg/ml. The r^2 of the calibration curve was 0.998.

Extensive phytochemical studies have been carried out on various parts of *A. muricata* in which 212 secondary metabolites such as acetogenins, alkaloids, phenol compounds, and megastigmanes are isolated and characterized (Coria-Téllez, *et al.,* 2018). Annonaceous acetogenins, a unique group formed by derivatives of long-chain fatty acids derived from the polyketide pathway and found in the *Annonaceae* family, are found in *A. muricata* leaves (Sun *et al*., 2016). The result of the present study confirmed previous studies, showing phenol or flavonoid compounds in *A. muricata* leaf extract.

In the present study, carbopol-940 was selected as the gelling agent due to its strength, clarity, temperature stability, and relatively small amount (0.5–5%) for the purpose of dermatological products (Bettini & Cocconi, 2001). As a result, carbopol-940 was used in several sustained-release preparations (Md *et al*., 2020; Newton, *et al.,* 2014). Nevertheless, the usage of hydrogels is hampered by their macroscopic size and the rapid elution of medicines using the inflated gel network (Schwall & Banerjee, 2009). In this study, the components of the gel were released slowly (Figure 5A), indicating the ability of the formulation to release the active compound.

Initially, the release rate of the formulation was relatively high allegedly due to the incomplete gel formation, but the rate was slower following the completion of gel formation (Figure 5A). The release profiles exhibited an inflexion point that indicated the gel formation on the diffusion membrane in the donor compartment of the diffusion cell. During the gel formation, formulation was converted into the gel phase and the drug release was slower. The results showed that the formed gels could retain *A. muricata* extract during the process.

Previous study suggested that the zinc acetate reacted with an equivalent amount of ammonium hydroxide solution and formed a zinc hydroxide precipitate—which dissolved to form ammonium zincate in the presence of an excess amount of ammonium hydroxide solution. The process of heating while stirring led ammonium zincate to transform into ZnO nanoparticles (Ismail *et al*., 2021). Similar to Ismail *et al*. (2021), this study found the cross-linking between Carbopol-940 and ZnO as confirmed by the FTIR spectra. The FTIR profile (Figure 5B) blue shift of the bending hydroxyl group of carbopol-940 from 1600 cm^{-1} towards higher energy, indicating the cross-linking reaction between carbopol-940 and zinc acetate.

Additionally, the XRD spectra of two standards (nZPs and Zn(OH)2) were compared to identify the presence of ZnO precipitates. The XRD was used to determine the crystal structure and phase identification of a material (Jendrzejewska, 2020). The comparison of XRD spectra of nZPs and

Zn(OH)2 standards found the presence of ZnO precipitates in the sample. It might be attributed to the synthesis method, impurities in the starting materials, or reaction between components.

Based on the parameters (Table I), our formula demonstrates the marketability of gel preparation**.** It shows the thermodynamic stability that occurs when a system is in its lowest energy level or chemically compatible with its environment (Md *et al*., 2020). Nevertheless, the PDI value of the gel displays non-uniformity of particle size, even though the other parameters meet the requirements. Moreover, the surface charge of the drop*et al*so directly influences nanoparticle stability. An increase in the electrostatic repulsion forces between droplets will decrease the possibility of coalescence while globules will be uniformly distributed (Sobhani *et al*., 2015). In the present study, the zeta potential of the optimized gel was -60. This negative value is possibly caused by the presence of the anionic group on carboxylic acids of the carbopol-940 (Md *et al*., 2020). In addition, nanoparticles with negative charge on the surface of the droplets show better skin penetration while keeping the droplet size at its minimum value (Rai, Mishra, Yadav, & Yadav, 2018).

Chitosan is a type of polysaccharide derived from chitin. Polysaccharides are non-toxic and biocompatible natural substances. They have various molecular weights and functional groups that can be chemically modified. They increase the water solubility of the conjugated hydrophobic moiety and are effective for drug delivery and other biomedical applications (Basu, Kunduru, Abtew, & Domb, 2015). The extract of *A. muricata* leaves showed a positive charge, while chitosan showed a negative charge (Figure 3C), making them a suitable combination for nanoparticle formation (Alishahi *et al*., 2011). Nanoparticles formed by mechanical stirring at room temperature resulted in the separation of chitosan into spherical particles of 358.45 ± 11.3 nm in size with negative surface charge. Essentially, the preparation of chitosan-TPP/*A. muricata* nanoparticles were successfully done through ionotropic gelation between the positively charged amino groups of chitosan-TPP and nALE, with constant stirring at room temperature for 1 h.

CONCLUSION

The innovative nanoparticle hydrogel formulation containing nanoparticles from *A. muricata* leaf extract (nALE) and zinc oxide nanoparticles (ZNPs) has been successfully prepared for the purpose of transdermal application. The formulated nano-gel is optimized for homogeneity, particle size, pH, in vitro drug release, skin irritation test, spreadability, and viscosity. In overall, the formulation has the potential for delivering and enhancing the efficacy of medicinal plants and their active compounds. Further study is needed to investigate the chemical stability of active compounds in *A. muricata* leaf extract, while in vivo study is required to assess the efficiency of the formulation as wound healing.

ACKNOWLEDGMENTS

We would like to express our gratitude to the Ministry of Higher Education for supporting this project (Applied research reference number 1868/1867/E4/AK.04/2021 and Contract number for research 312/E4.1/AK.04.PT/2021).

CONFLICT OF INTEREST

The authors declare no conflict of interest.

REFERENCES

Abdellatif, A. A. H., El-Telbany, D., Zayed, G., & Al-Sawahli, M. (2018). Hydrogel Containing PEG-Coated Fluconazole Nanoparticles with Enhanced Solubility and Antifungal Activity. *Journal of Pharmaceutical Innovation, 14*. doi:10.1007/s12247-018-9335-z

Agu, K. C., & Okolie, P. N. (2017). Proximate composition, phytochemical analysis, and in vitro antioxidant potentials of extracts of Annona muricata (Soursop). *Food science & nutrition, 5*(5), 1029-1036. doi:10.1002/fsn3.498

Alishahi, A., Mirvaghefi, A., Tehrani, M., Farahmand, H., Koshio, S., Dorkoosh, F., & Elsabee, M. Z. (2011). Chitosan nanoparticle to carry vitamin C through the gastrointestinal tract and induce the non-specific immunity system of rainbow trout (Oncorhynchus mykiss). *Carbohydrate Polymers, 86*(1), 142-146.

Ansari, S. H., Islam, F., & Sameem, M. (2012). Influence of nanotechnology on herbal drugs: A Review. *Journal of advanced pharmaceutical technology & research, 3*(3), 142-146. doi:10.4103/2231-4040.101006

Basu, A., Kunduru, K. R., Abtew, E., & Domb, A. J. (2015). Polysaccharide-Based Conjugates for Biomedical Applications. *Bioconjug Chem, 26*(8), 1396-1412. doi:10.1021/acs.bioconjchem.5b00242

Batheja, P., Sheihet, L., Kohn, J., Singer, A. J., & Michniak-Kohn, B. (2011). Topical drug delivery by a polymeric nanosphere gel: formulation optimization and in vitro and in vivo skin distribution studies. *Journal of controlled release, 149*(2), 159-167.

Bettini, R., & Cocconi, D. (2001). Handbook of Pharmaceutical Excipients, Third Edition: Arthur H. Kibbe (ed.), Pharmaceutical Press, London, 2000, 665 pp. *Journal of controlled release, 71*, 352–353.

Chang, C. C., Yang, M. H., Wen, H. M., & Chern, J. C. (2002). Estimation of Total Flavonoid Content in Propolis by Two Complementary Colorimetric Methods. *Journal of Food and Drug Analysis, 10*, 178-182.

Coria-Téllez, A. V., Montalvo-Gónzalez, E., Yahia, E. M., & Obledo-Vázquez, E. N. (2018). Annona muricata: A comprehensive review on its traditional medicinal uses, phytochemicals, pharmacological activities, mechanisms of action and toxicity. *Arabian Journal of Chemistry, 11*(5), 662-691.

Gato, K., Fujii, M. Y., Hisada, H., Carriere, J., Koide, T., & Fukami, T. (2020). Molecular state evaluation of active pharmaceutical ingredients in adhesive patches for transdermal drug delivery. *Journal of Drug Delivery Science and Technology, 58*, 101800. doi:https://doi.org/10.1016/j.jddst.2020.101800

Gupta, M., Mahajan, V. K., Mehta, K. S., & Chauhan, P. S. (2014). Zinc therapy in dermatology: a review. *Dermatology research and practice, 2014*, 709152-709152. doi:10.1155/2014/709152

Henzel, J. H., DeWeese, M. S., & Lichti, E. L. (1970). Zinc concentrations within healing wounds. Significance of postoperative zincuria on availability and requirements during tissue repair. *Arch Surg, 100*(4), 349-357. doi:10.1001/archsurg.1970.01340220025005

Ismail, S. H., Hamdy, A., Ismail, T. A., Mahboub, H. H., Mahmoud, W. H., & Daoush, W. M. (2021). Synthesis and Characterization of Antibacterial Carbopol/ZnO Hybrid Nanoparticles Gel. *Crystals, 11*(9). doi:10.3390/cryst11091092

Iswanti, F. C., Nurulita, I., Djauzi, S., Sadikin, M., Witarto, A. B., & Yamazaki, T. (2019). Preparation, characterization, and evaluation of chitosan-based nanoparticles as CpG ODN carriers. *Biotechnology & Biotechnological Equipment, 33*(1), 390-396. doi:10.1080/13102818.2019.1578690

Jendrzejewska, I. (2020). Application of X-Ray Powder Diffraction for Analysis of Selected Dietary Supplements Containing Magnesium and Calcium. *Frontiers in Chemistry, 8*. doi:10.3389/fchem.2020.00672

Joshi, M., & Patravale, V. (2006). Formulation and Evaluation of Nanostructured Lipid Carrier (NLC)–based Gel of Valdecoxib. *Drug development and industrial pharmacy, 32*, 911-918. doi:10.1080/03639040600814676

Kalaiselvi, M., Duraisamy, G., & Uma, C. (2012). Occurrence of Bioactive compounds in Ananus comosus (L.): A quality Standardization by HPTLC. *Asian Pacific Journal of Tropical Biomedicine, 2*, S1341–S1346. doi:10.1016/S2221-1691(12)60413-4

Kesarwani, K., Gupta, R., & Mukerjee, A. (2013). Bioavailability enhancers of herbal origin: an overview. *Asian Pac J Trop Biomed, 3*(4), 253-266. doi:10.1016/s2221-1691(13)60060-x

Khan, I., Saeed, K., & Khan, I. (2019). Nanoparticles: Properties, applications and toxicities. *Arabian Journal of Chemistry, 12*(7), 908-931. doi:https://doi.org/10.1016/j.arabjc.2017.05.011

Kim, G.-T., Tran, N. K. S., Choi, E.-H., Song, Y.-J., Song, J.-H., Shim, S.-M., & Park, T.-S. (2016). Immunomodulatory Efficacy of Standardized Annona muricata (Graviola) Leaf Extract via Activation of Mitogen-Activated Protein Kinase Pathways in RAW 264.7 Macrophages. *Evidence-Based Complementary and Alternative Medicine, 2016*, 2905127. doi:10.1155/2016/2905127

Md, S., Alhakamy, N. A., Aldawsari, H. M., Kotta, S., Ahmad, J., Akhter, S., . . . Sivakumar, P. M. (2020). Improved Analgesic and Anti-Inflammatory Effect of Diclofenac Sodium by Topical Nanoemulgel: Formulation Development—In Vitro and In Vivo Studies. *Journal of Chemistry, 2020*, 4071818. doi:10.1155/2020/4071818

Moghadamtousi, S. Z., Rouhollahi, E., Hajrezaie, M., Karimian, H., Abdulla, M. A., & Kadir, H. A. (2015). Annona muricata leaves accelerate wound healing in rats via involvement of

Hsp70 and antioxidant defence. *Int J Surg, 18*, 110-117. doi:10.1016/j.ijsu.2015.03.026

Moghadamtousi, Z S., Abdul Kadir, H., Hassandarvish, P., Tajik, H., Abubakar, S., & Zandi, K. (2014). A Review on Antibacterial, Antiviral, and Antifungal Activity of Curcumin. *BioMed Research International, 2014*, 186864. doi:10.1155/2014/186864

Moghimi, S. M., Hunter, A. C., & Murray, J. C. (2005). Nanomedicine: current status and future prospects. *Faseb j, 19*(3), 311-330. doi:10.1096/fj.04-2747rev

Mugiyanto, E., Cahyanta, A. N., Putra, I. M. A. S., Setyahadi, S., & Simanjuntak, P. (2019). Identifying active compounds of soursop ethanolic fraction as α-glucosidase inhibitor. *Pharmaciana, 9*(2), 191-200.

Najihah, N., Ya'akob, H., & Mohamad Rosdi, M. N. (2016). Acetogenins of Annona muricata leaves: Characterization and potential anticancer study. *Integrative Cancer Science and Therapeutics, 3*. doi:10.15761/ICST.1000202

Newton, M., Maheshbabu, C., Kumar, N., & Kumar, R. (2014). Effect of Carbopol 940 on Drug Release Profile and Floating Characteristics of Floating Drug Delivery System of Amoxicillin Trihydrate Using HPMC Different Grades. Journal of Applied Biopharmaceutics and Pharmacokinetics, Volume 2, No. 1, June 2014. *Journal of Applied Biopharmaceutics and Pharmacokinetics, 2*. doi:10.14205/2309-4435.2014.02.01.4

Ogbu, I. M., & Ajiwe, V. I. E. (2016). FTIR studies of thermal stability of the oils and methyl esters from Afzelia africana and Hura crepitans seeds. *Renewable Energy, 96*, 203-208. doi:https://doi.org/10.1016/j.renene.2016.04.055

Padmini, C., Samarasekera, R., & Pushpakumara, D. (2015). Antioxidant capacity and total phenol content of Sri Lankan Annona muricata L. *Tropical Agricultural Research, 25*, 252. doi:10.4038/tar.v25i2.8146

Patra, J. K., Das, G., Fraceto, L. F., Campos, E. V. R., Rodriguez-Torres, M. D. P., Acosta-Torres, L. S., . . . Shin, H. S. (2018). Nano based drug delivery systems: recent developments and future prospects. *J Nanobiotechnology, 16*(1), 71. doi:10.1186/s12951-018-0392-8

Rai, V. K., Mishra, N., Yadav, K. S., & Yadav, N. P. (2018). Nanoemulsion as pharmaceutical carrier for dermal and transdermal drug delivery: Formulation development, stability issues, basic considerations and applications. *J Control Release, 270*, 203-225. doi:10.1016/j.jconrel.2017.11.049

Robinson, M. K., Parsell, K. W., Breneman, D. L., & Cruze, C. A. (1991). Evaluation of the primary skin irritation and allergic contact sensitization potential of transdermal triprolidine. *Fundamental and Applied Toxicology, 17*(1), 103-119. doi:https://doi.org/10.1016/0272-0590(91)90243-W

Roohani, N., Hurrell, R., Kelishadi, R., & Schulin, R. (2013). Zinc and its importance for human health: An integrative review. *J Res Med Sci, 18*(2), 144-157.

Schwall, C. T., & Banerjee, I. A. (2009). Micro- and Nanoscale Hydrogel Systems for Drug Delivery and Tissue Engineering. *Materials, 2*(2), 577-612. doi:10.3390/ma2020577

Sobhani, H., Tarighi, P., Ostad, S. N., Shafaati, A., Nafissi-Varcheh, N., & Aboofazeli, R. (2015). Formulation Development and Toxicity Assessment of Triacetin Mediated Nanoemulsions as Novel Delivery Systems for Rapamycin. *Iran J Pharm Res, 14*(Suppl), 3-21.

Sun, S., Liu, J., Zhou, N., Zhu, W., Dou, Q. P., & Zhou, K. (2016). Isolation of three new annonaceous acetogenins from Graviola fruit (Annona muricata) and their anti-proliferation on human prostate cancer cell PC-3. *Bioorganic & medicinal chemistry letters, 26*(17), 4382-4385.

Sungthongjeen, S., Pitaksuteepong, T., Somsiri, A., & Sriamornsak, P. (1999). Studies on pectins as potential hydrogel matrices for controlled-release drug delivery. *Drug Dev Ind Pharm, 25*(12), 1271-1276. doi:10.1081/ddc-100102298

Talam, S., Karumuri, S. R., & Gunnam, N. (2012). Synthesis, Characterization, and Spectroscopic Properties of ZnO Nanoparticles. *ISRN Nanotechnology, 2012*, 372505. doi:10.5402/2012/372505

Wang, Z., Li, H., Tang, F., Ma, J., & Zhou, X. (2018). A Facile Approach for the Preparation of Nano-size Zinc Oxide in Water/Glycerol with Extremely Concentrated Zinc Sources. *Nanoscale research letters, 13*(1), 202-202.

WHO. (2019). *WHO global report on traditional and complementary medicine 2019*. Retrieved from